

# GPX7 reduces chondrocyte inflammation and extracellular matrix degradation triggered by IL-1 $\beta$ , via a mechanism mediated by ferroptosis

BOYUAN CHEN<sup>1</sup>, WEIHAO FU<sup>2</sup>, CHUNYANG JIE<sup>1</sup>, GUOXIU ZHANG<sup>3</sup>,  
ZHEN LI<sup>1</sup>, YIHAI LIU<sup>1</sup> and SHIBO ZHOU<sup>1</sup>

<sup>1</sup>Department of Physical Education, Henan University of Science and Technology, Luoyang, Henan 471023, P.R. China;

<sup>2</sup>Integrative Exercise Physiology Laboratory, Department of Physical Education, Jeonbuk National University, Jeonju 54896, Republic of Korea; <sup>3</sup>Department of General Medicine, The First Affiliated Hospital of

Henan University of Science and Technology, Luoyang, Henan 471023, P.R. China

Received February 22, 2024; Accepted April 23, 2024

DOI: 10.3892/mmr.2024.13242

**Abstract.** During osteoarthritis (OA), chondrocytes become highly active, with increased matrix synthesis and inflammatory cytokine-induced catabolic pathways. Early intervention strategies targeting pathological changes may attenuate or halt disease progression. The present study aimed to reveal the role of glutathione peroxidase (GPX)7 in OA. For this purpose, a research model was established by inducing C28/I2 human chondrocytes with interleukin (IL)-1 $\beta$ , and the expression level of GPX7 was determined. To explore its roles, C28/I2 cells were transfected to gain GPX7 overexpression. The effects of GPX7 overexpression on intracellular inflammation, extracellular matrix (ECM) degradation, apoptosis and ferroptosis were then evaluated. In addition, the cells were treated with the ferroptosis inducer, erastin, and its effects on the aforementioned phenotypes were assessed. The level of GPX7 was decreased in response to IL-1 $\beta$  treatment, and GPX7 overexpression suppressed cellular inflammation, ECM degradation and apoptosis. Moreover, the reduction of lipid peroxidation, ferrous ions and transferrin indicated that GPX7 overexpression inhibited ferroptosis. Subsequently, inflammation, ECM degradation and apoptosis were found to be promoted in the cells upon treatment with erastin. These findings suggested that the regulatory role of GPX7 may be mediated by a pathway involving ferroptosis. On the whole, the present study revealed that GPX7 reduces IL-1 $\beta$ -induced chondrocyte inflammation, apoptosis and ECM degradation partially through a mechanism involving ferroptosis. The results of the present study lay

a theoretical foundation for subsequent OA-related research and may enable the development of translational strategies for the treatment of OA.

## Introduction

Osteoarthritis (OA) has a high clinical incidence rate and is a common chronic degenerative joint disease (1). Musculoskeletal disorders, including OA, are the leading cause of disability worldwide and significantly contribute to increased health care costs (2). There are a number of risk factors for the development of OA, including previous joint injury, obesity, genetics, sex and anatomical factors related to joint shape and alignment; however, the most prominent risk factor is an increasing age (3). Advanced-stage OA often requires joint replacement to relieve pain and disability, and the number of knee replacement surgeries has markedly increased over the past 20 years. The aging of the population will increase the number of older adults who are disabled by OA and require joint replacements (4). OA that occurs in young individuals is usually caused by a previous joint injury, such as an anterior cruciate ligament or meniscal tear, which is common in athletes and induces the early onset of OA in patients (5). During OA, chondrocytes become highly active, with increased matrix synthesis and inflammatory cytokine-induced catabolic pathways (6). Early intervention strategies targeting pathological changes may attenuate or halt disease progression.

Glutathione peroxidase (GPX) is a family of antioxidant enzymes with eight types, GPX1-8. Together with superoxide dismutase and catalase, GPX forms an enzymatic antioxidant system that reduces reactive oxygen species (ROS) (7). GPX7 is mainly located in the endoplasmic reticulum (ER) and has two unique ER-secreted proteins, namely the N-terminal ER signal peptide and the C-terminal atypical KDEL sequence (8). Unlike other family members, GPX7 does not apply GSH as a substrate to participate in redox reactions, but promotes signal transduction and release by targeting proteins, such as GRP78 (9). In osteoporosis, GPX7 promotes osteoblastogenesis

---

*Correspondence to:* Dr Boyuan Chen, Department of Physical Education, Henan University of Science and Technology, 263 Kaiyuan Avenue, Luoyang, Henan 471023, P.R. China  
E-mail: boyuanchendr@163.com

**Key words:** chondrocyte, extracellular matrix, ferroptosis, glutathione peroxidase, osteoarthritis

in bone marrow-derived mesenchymal stem cells by inhibiting ER stress, and can also regulate bone mass and bone turnover by blocking signals through the gp130 transducer protein (10). It has been demonstrated that GPX7 overexpression in hepatocytes inhibits ROS production and reduces the expression of pro-fibrotic and pro-inflammatory genes, improving non-alcoholic steatohepatitis (11). Furthermore, GPX7 protects cells from oxidative stress during epidermal keratinogenesis (12). Nevertheless, the role of GPX7 in OA remains unclear.

Previous studies have indicated that D-mannose alleviates the progression of OA by inhibiting the HIF-2 $\alpha$ -mediated sensitivity of chondrocytes to ferroptosis (13), while GPX7 knockdown enhances ferroptosis in glioma (14). Therefore, it was hypothesized that in OA, increasing GPX7 expression could alleviate the progression of the disease by inhibiting ferroptosis. The present study established a research model by inducing chondrocytes with interleukin (IL)-1 $\beta$ , and explored the effects of GPX7 on intracellular inflammation, extracellular matrix (ECM) breakdown and ferroptosis by increasing intracellular GPX7 expression. The findings of the present study may lay a theoretical foundation for subsequent OA-related research.

## Materials and methods

**Cells, cell culture and treatment.** The immortalized human chondrocytes, C28/I2 [cat. no. BFN60803901; BLUEFBIOLife Sciences; Qingqi (Shanghai) Biotechnology Development Co., Ltd.], were cultured in Dulbecco's modified Eagle's medium (DMEM) supplemented with 10% fetal bovine serum and 1% penicillin/streptomycin under 5% CO<sub>2</sub> at 37°C. The C28/I2 cells were stimulated with IL-1 $\beta$  (10 ng/ml, MilliporeSigma) for 24 h to mimic OA *in vitro* (15). Additionally, to explore the mediating effects of ferroptosis, the C28/I2 cells were pre-treated with erastin (5  $\mu$ M, Selleck Chemicals), a type of ferroptosis inducer (16), for 24 h.

**Cell transfection.** The C28/I2 cells were transfected with plasmids [cat. no. GM-1013P001, Genomeditech (Shanghai) Co., Ltd.] carrying GPX7 to achieve gene overexpression. The cells transfected with empty vectors were regarded as the negative control (named oe-NC). The C28/I2 cells were seeded in a six-well plate the day prior to transfection, 5  $\mu$ g plasmids were mixed with Lipofectamine 3000<sup>®</sup> transfection reagent (Thermo Fisher Scientific, Inc.) and were then added to the wells. The cells were harvested following 48 h of transfection at 37°C to assess the transfection efficiency.

**Western blot analysis.** The concentration of protein extracted from the C28/I2 cells with RIPA (Shanghai Maokang BioTec Co., Ltd.) was determined using a Nanodrop 2000 spectrophotometer (Thermo Fisher Scientific, Inc.). These proteins (20  $\mu$ g/lane) were subsequently resolved on 15% sodium dodecyl sulfate-polyacrylamide gels and transferred onto PVDF membranes (MilliporeSigma). The membranes were blocked at room temperature with 5% skimmed milk for 1 h, incubated at 4°C overnight with primary antibodies [anti-GPX7 (cat. no. 13501-1-AP; Proteintech Group, Inc.), aggrecan (cat. no. MA3-16888; Invitrogen), collagen II (cat. no. PA5-99159; Invitrogen; Thermo Fisher

Scientific, Inc.), MMP13 (cat. no. 18165-1-AP; Proteintech Group, Inc.), A disintegrin and metalloproteinase with thrombospondin motifs 5 (ADAMTS5; cat. no. PA5-32142; 3,000 dilution; Invitrogen; Thermo Fisher Scientific, Inc.), Bcl2 (cat. no. 66799-1-Ig; Proteintech Group, Inc.), Bax (cat. no. 50599-2-Ig; 8,000 dilution; Proteintech Group, Inc.), cleaved caspase-3 (cat. no. 25128-1-AP; Proteintech Group, Inc.), caspase-3 (cat. no. 19677-1-AP; Proteintech Group, Inc.), cleaved caspase-9 (cat. no. PA5-77889; Invitrogen; Thermo Fisher Scientific, Inc.), caspase-9 (cat. no. 10380-1-AP; Proteintech Group, Inc.), ferritin heavy chain 1 (FTH1; cat. no. 11682-1-AP; Proteintech Group, Inc.), GPX4 (cat. no. 67763-1-Ig; Proteintech Group, Inc.), transferrin (Tf; cat. no. 17435-1-AP; Proteintech Group, Inc.) and GAPDH (cat. no. 60004-1-Ig; 200,000 dilution; Proteintech Group, Inc.); and then incubated with HRP-linked goat secondary antibody (cat. no. SA00001-1 and SA00001-2; 10,000 dilution; Proteintech Group, Inc.) for 1.5 h at 37°C. Unless otherwise stated, antibodies were diluted a 1,000-fold. The bands were visualized using enhanced chemifluorescence substrate (GE Healthcare; Cytiva) and semi-quantified using ImageJ software (version 1.53; National Institutes of Health).

**Reverse transcription-quantitative PCR (RT-qPCR).** Complementary DNA was acquired by converting total RNA from the C28/I2 cells (extracted with TRIzol; Invitrogen;) using the Evo M-MLV reverse transcription assay kit [Accurate Biology (Changsha) Co., Ltd] according to the manufacturer's instructions. qPCR was performed using the QuantiTect SYBR-Green PCR kit (Qiagen GmbH). qPCR was performed in a total volume of 20- $\mu$ l reaction system, containing 10  $\mu$ l Master Mix, 10 ng DNA template and 500 nM specific forward and reverse primers for GPX7. The thermocycling conditions were as follows: 95°C for 15 min, and 40 cycles of 94°C for 15 sec, 55°C for 30 sec and 72°C for 30 sec. The expression levels of mRNA were quantified using the 2<sup>- $\Delta\Delta$ C<sub>q</sub></sup> method (17) and normalized to the levels of actin. Primer sequences were as follows: GPX7 forward, 5'-TACGACTTCAAGGCGGTC AA-3' and reverse, 5'-CCACCAGGGACACCGATCC-3'; and actin forward, 5'-CTTCGCGGGCGACGAT-3' and reverse, 5'-CCACATAGGAATCCTTCTGACC-3'.

**ELISA.** The levels of TNF- $\alpha$  and IL-6 were detected using ELISA kits (cat. nos. PT518 and PI330; Beyotime Institute of Biotechnology) to assess the degree of inflammation. The supernatant of C28/I2 cells was obtained by centrifugation at 2,000 x g, 4°C for 10 min. The collected supernatant was incubated at room temperature with biotin-labeled antibodies for 1 h, avidin-peroxidase complex for 20 min, TMB chromogenic solution for 20 min, and stop solution provided with the kit in sequence. Absorbance at 450 nm was measured using a microplate reader (Molecular Devices, LLC).

**TUNEL assay.** TUNEL assay was performed to determine apoptosis using a TUNEL kit (cat. no. C1086; Beyotime Institute of Biotechnology). The C28/I2 cells were fixed with 4% paraformaldehyde for 30 min and incubated with PBS containing 0.3% Triton X-100 for 5 min at room temperature. The C28/I2 cells were then incubated at 37°C with TUNEL working fluid for 1 h in the dark. Microcopies

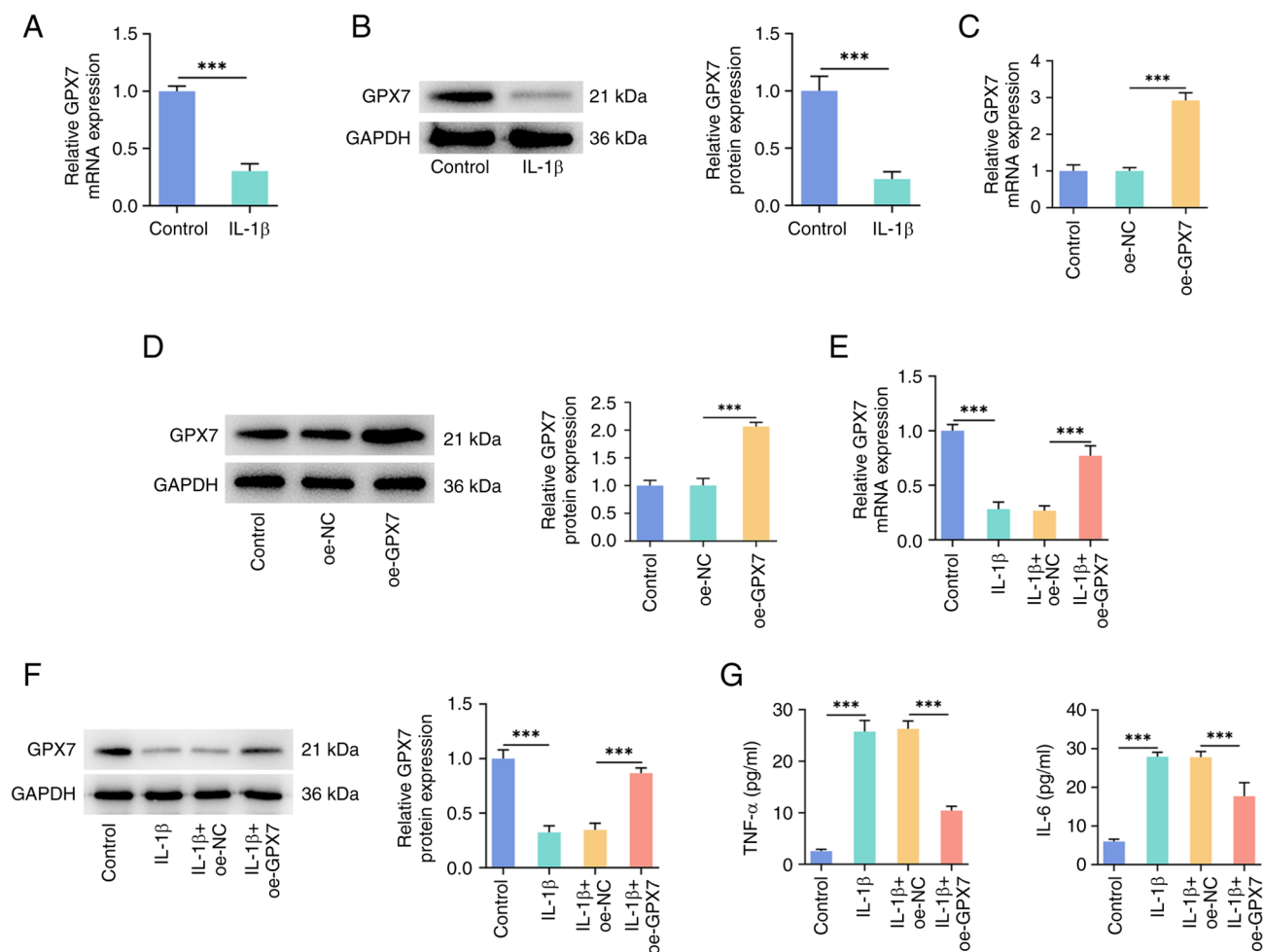


Figure 1. GPX7 overexpression inhibits IL-1 $\beta$ -induced chondrocyte inflammation. The results of (A) RT-qPCR and (B) western blot analysis demonstrated the mRNA and protein level of GPX7 in C28/I2 cells in response to IL-1 $\beta$  treatment. (C) RT-qPCR and (D) western blot analysis were used to determine the GPX7 level to assess the transfection efficacy. The results of (E) RT-qPCR and (F) western blot analysis demonstrated the mRNA and protein level of GPX7 in the cells treated with IL-1 $\beta$ . (G) ELISA was used to measure the levels of inflammatory factors. \*\*\*P<0.001. GPX7, glutathione peroxidase 7; RT-qPCR, reverse transcription-quantitative PCR; oe, overexpression; NC, negative control.

were captured under a fluorescence microscope (Olympus Corporation).

**C11-BODIPY.** The C11 BODIPY probe (cat. no. ajci64572; Amgicam; Wuhan Anjiekai Biomedical Science and Technology Co., Ltd.) was used to indicate lipid peroxidation. The C28/I2 cells were washed with PBS thrice and incubated with C11 BODIPY for 30 min. Following washing with PBS twice, the cells were observed under a fluorescence microscope (Olympus Corporation).

**FerroOrange.** The ferrous iron level in the C28/I2 cells was determined using FerroOrange probes (cat. no. F374; Dojindo Laboratories, Inc.). The cells were washed with PBS thrice and incubated at 37°C with FerroOrange for 30 min. Following washing with PBS twice, the cells were observed under a fluorescence microscope (Olympus Corporation).

**Statistical analysis.** Data are presented as the mean  $\pm$  standard deviation and were analyzed using GraphPad 8.0 software (Dotmatics). Significant differences between two groups were determined using a two-tailed unpaired Student's t test and

those between multiple groups were determined using one-way ANOVA followed by Tukey's post hoc test. A value of P<0.05 was considered to indicate a statistically significant difference.

## Results

**GPX7 overexpression inhibits IL-1 $\beta$ -induced chondrocyte inflammation.** The results of RT-qPCR and western blot analysis demonstrated that the GPX7 level was decreased in chondrocytes in response to IL-1 $\beta$  treatment, compared with the control group (Fig. 1A and B). In order to explore the specific role of GPX7 in chondrocytes, the C28/I2 cells were transfected with plasmids overexpressing GPX7. The results of RT-qPCR and western blot analysis confirmed that the GPX7 level in the oe-GPX7 group was significantly higher than that in the oe-NC group, indicating that the transfection was successful (Fig. 1C and D). Similarly, following treatment with IL-1 $\beta$ , the expression of GPX7 in the oe-GPX7 group was higher than that in the oe-NC group (Fig. 1E and F). In addition, ELISA was used to measure the levels of inflammatory factors to evaluate the degree of the inflammatory response in cells. The levels of TNF- $\alpha$  and IL-6 in the cell supernatant

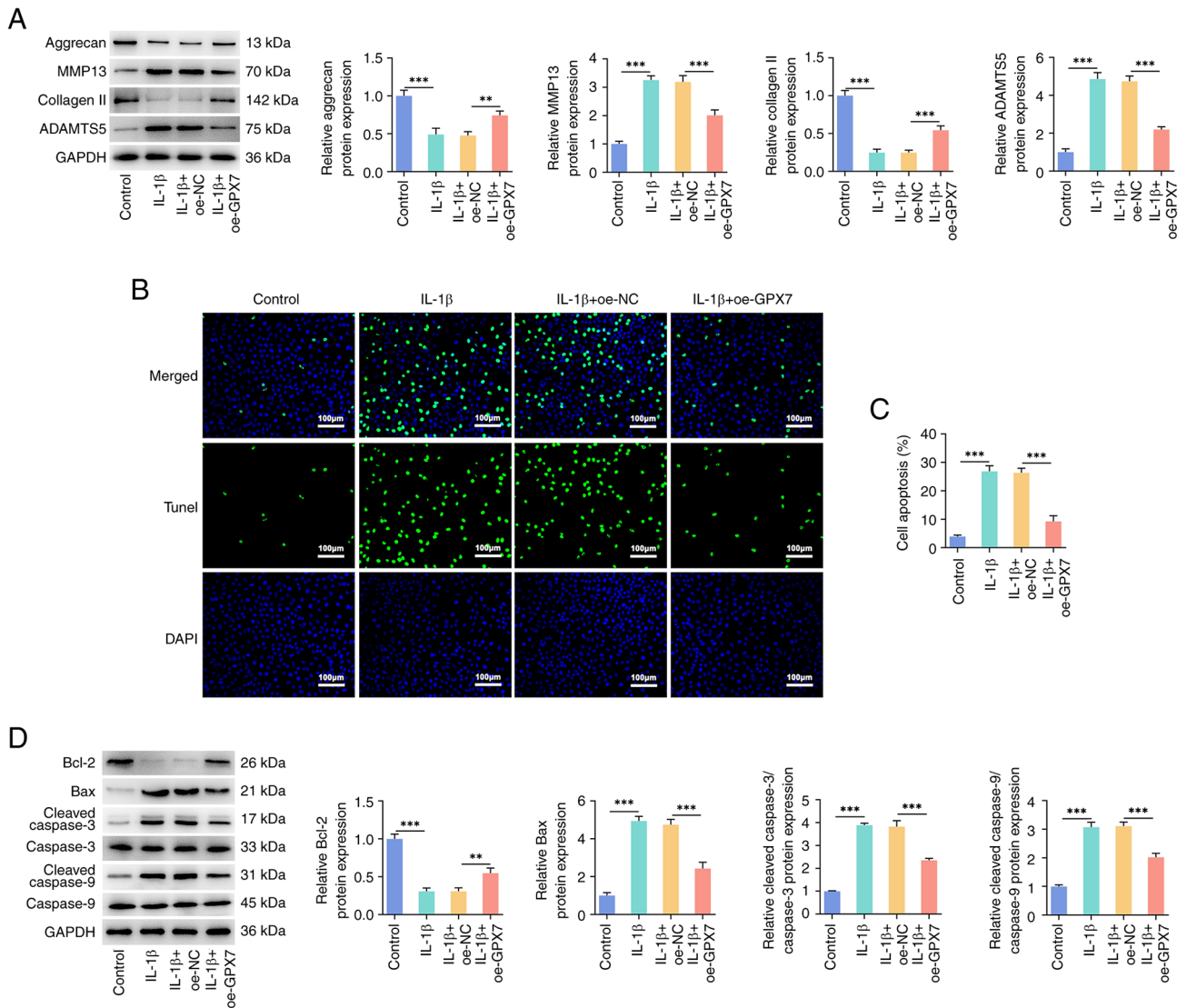


Figure 2. GPX7 overexpression inhibits IL-1 $\beta$ -induced cartilage ECM degradation and apoptosis. (A) Western blot analysis was used to determine the levels of extracellular matrix-related proteins in the cells. (B and C) TUNEL staining reflected the degree of cell apoptosis. (D) Western blot analysis demonstrated the levels of apoptosis-related proteins. \*\* $P < 0.01$  and \*\*\* $P < 0.001$ . GPX7, glutathione peroxidase 7; oe, overexpression; NC, negative control.

were significantly increased upon IL-1 $\beta$  treatment, and a similar increase was observed in the IL-1 $\beta$  + oe-NC group. Compared with the IL-1 $\beta$  + oe-NC group, the levels of TNF- $\alpha$  and IL-6 decreased in the IL-1 $\beta$  + oe-GPX7 group (Fig. 1G).

*GPX7 overexpression inhibits IL-1 $\beta$ -induced cartilage ECM degradation and apoptosis.* Western blot analysis was used to determine the levels of ECM-related proteins in the C28/I2 cells. In response to IL-1 $\beta$  treatment, the protein levels of aggrecan and collagen II in the cells decreased, while those of MMP13 and ADAMTS5 increased. Compared with the IL-1 $\beta$  + oe-NC group, GPX7 overexpression attenuated the decline in aggrecan and collagen II protein levels, and reduced MMP13 and ADAMTS5 protein accumulation (Fig. 2A). TUNEL staining indicated the trend of cell apoptosis, and the fluorescence increased upon IL-1 $\beta$  treatment, indicating an increased cell apoptosis. Notably, compared with the IL-1 $\beta$  + oe-NC group, the apoptosis of GPX7-overexpressing cells was significantly reduced following treatment with IL-1 $\beta$  (Fig. 2B and C). In addition, the levels of the pro-apoptotic

proteins, Bax, cleaved caspase-3/caspase-3 and cleaved caspase-9/caspase-9, were significantly increased in the cells under the influence of IL-1 $\beta$ , while the level of the anti-apoptotic protein, Bcl-2, decreased. The alterations in the levels of apoptosis-related proteins in the IL-1 $\beta$  + oe-GPX7 group were attenuated following the overexpression of GPX7, indicating the function of GPX7 in inhibiting apoptosis (Fig. 2D).

*GPX7 overexpression inhibits IL-1 $\beta$ -induced lipid peroxidation and ferroptosis in chondrocytes.* In the C11-BODIPY assay, the fluorescence in the IL-1 $\beta$  group increased, indicating that the level of lipid peroxidation increased, and GPX7 overexpression reduced the degree of this oxidation (Fig. 3A). IL-1 $\beta$  treatment also increased the ferrous ion levels in the C28/I2 cells, with the increase being less pronounced in the cells overexpressing GPX7 (Fig. 3B). By determining the levels of ferroptosis-related proteins, GPX7 overexpression was found to increase the FTH1 and GPX4 levels, and reduce the Tf protein levels, suggesting that it reversed IL-1 $\beta$ -induced ferroptosis (Fig. 3C).



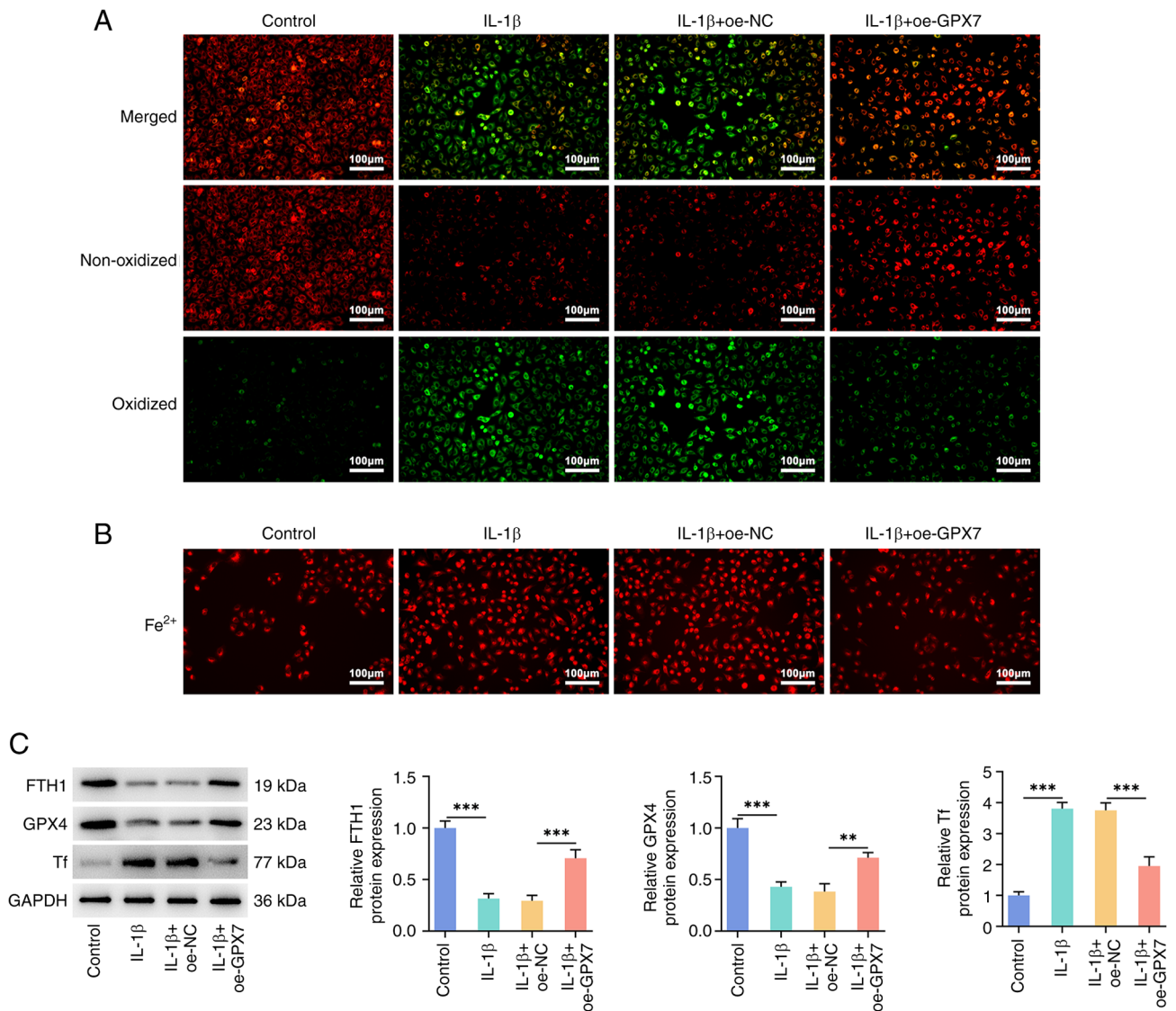


Figure 3. GPX7 overexpression inhibits IL-1 $\beta$ -induced lipid peroxidation and ferroptosis in chondrocytes. (A) C11-BODIPY assay indicated the level of lipid peroxidation. (B) FerroOrange assay indicated the ferrous ion levels. (C) Western blot analysis was used to determine the levels of ferroptosis-related proteins. \*\*P<0.01 and \*\*\*P<0.001. GPX7, glutathione peroxidase 7; oe, overexpression; NC, negative control.

*Effects of a ferroptosis inducer on the regulatory effects of GPX7 overexpression.* To verify the role of ferroptosis in the regulation of multiple phenotypes aforementioned in chondrocytes, the transfected cells were pre-treated with erastin followed by the treatment with IL-1 $\beta$ . Compared with the IL-1 $\beta$  + oe-GPX7 group, the addition of erastin increased the levels of the inflammatory factors, TNF- $\alpha$  and IL-6 (Fig. 4A). Furthermore, the addition of erastin inhibited the increase in the aggrecan and collagen II protein levels induced by the overexpression of GPX7, and elevated the levels of MMP13 and ADAMTS5 (Fig. 4B). These findings suggested that erastin promoted ECM degradation. The enhancement of TUNEL fluorescence in the erastin-treated group indicated that erastin reversed the inhibitory effects of GPX7 overexpression on cell apoptosis (Fig. 5A and B). This was supported by the increase in the levels of the apoptosis-related proteins, Bax, cleaved caspase-3/caspase-3 and cleaved caspase-9/caspase-9, and the decrease in the level of Bcl-2, as a consequence of erastin treatment (Fig. 5C).

## Discussion

The crux to the pathogenesis of OA is the destruction of cartilage cells, the degradation of cartilage ECM and the imbalance of the synthesis of subchondral bone components, which in turn cause cartilage tissue defects and ultimately lead to the occurrence of OA (18). In terms of genetic factors, the heritability of OA is enhanced within families, and the genetic probability of offspring developing OA is as high as 40-65% (19). At the molecular biological level, the pathogenesis of OA is closely related to various inflammatory factors, MMPs, signaling pathways and growth factors (20,21). Focusing on inflammatory factors, the present study found that GPX7 overexpression suppressed the TNF- $\alpha$  and IL-6 levels. The synthesis of these two factors is related to the development of arthritis and is considered a key drug target (22). Additionally, IL-6 is associated with aging (23), with the levels of IL-6 in the systemic circulation increasing with age, and being closely associated with the risk of OA progression.

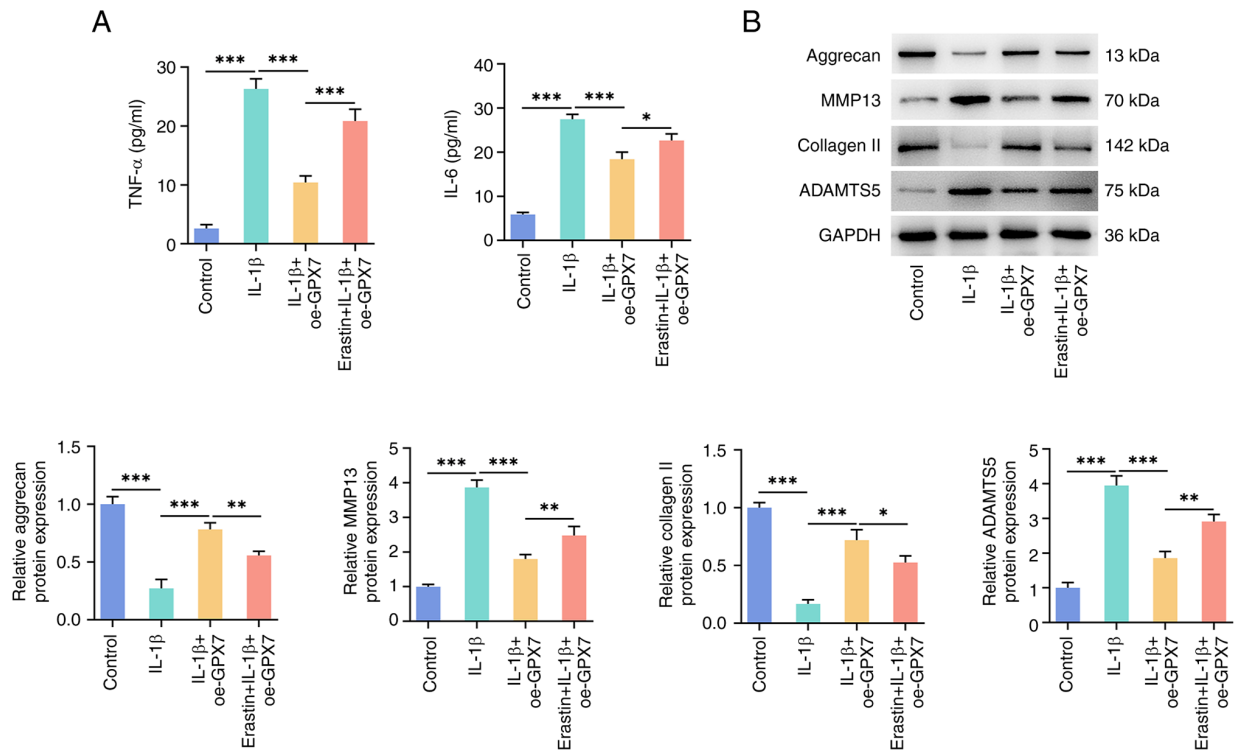


Figure 4. Effects of erastin on the regulation of GPX7 overexpression in inflammation and ECM degradation. (A) The transfected cells were pretreated with erastin followed by treatment with IL-1 $\beta$ . ELISA was used to determine the effects of erastin on the levels of inflammatory factors. (B) Western blot analysis was used to determine the effects of erastin on ECM degradation. \* $P < 0.05$ , \*\* $P < 0.01$  and \*\*\* $P < 0.001$ . GPX7, glutathione peroxidase 7; ECM, extracellular matrix; oe, overexpression; NC, negative control.

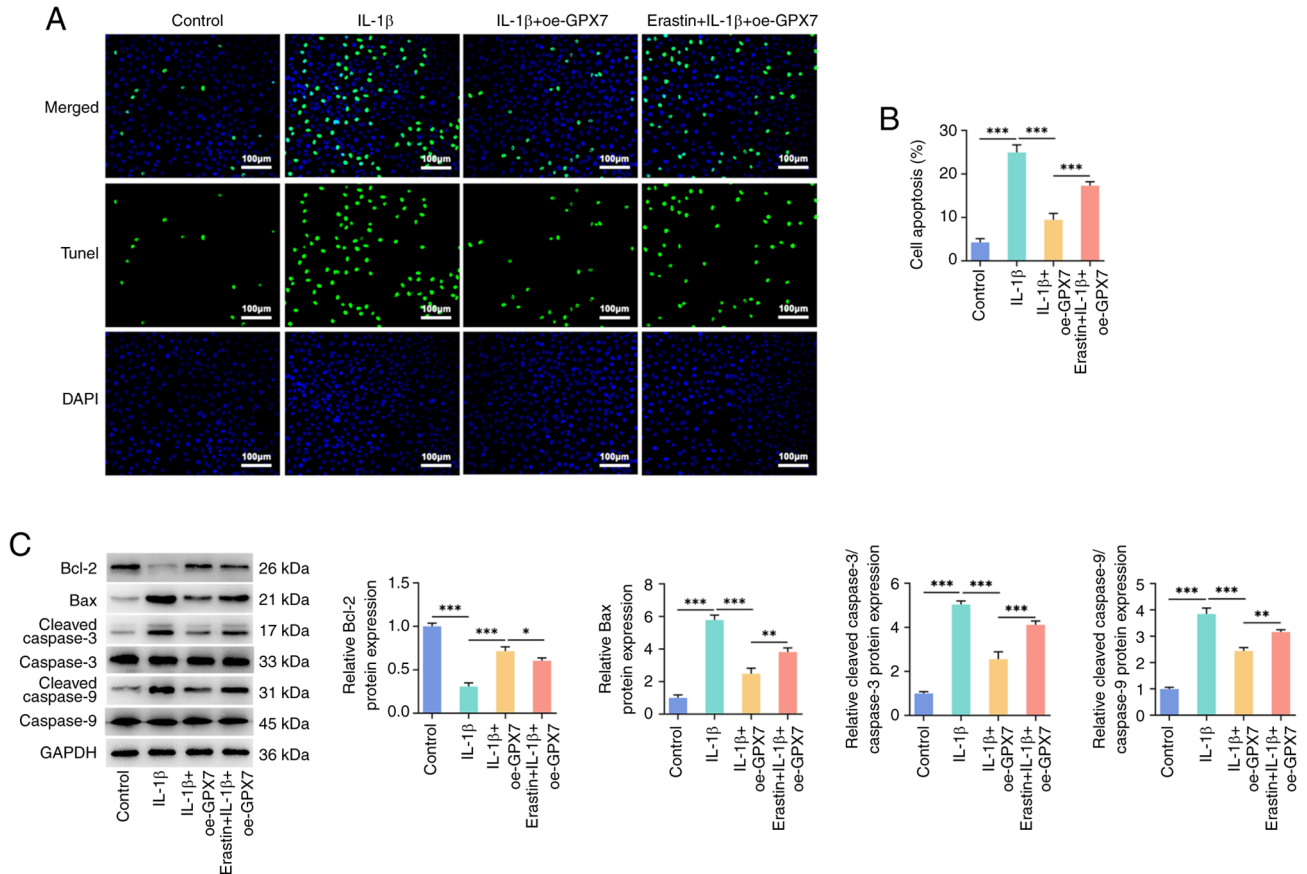


Figure 5. Effects of erastin on the regulation of GPX7 overexpression in apoptosis. (A and B) TUNEL assay was used to determine the effects of erastin on the apoptosis. (C) Western blot analysis was used to determine the effects of erastin on the levels of apoptosis-related proteins. \* $P < 0.05$ , \*\* $P < 0.01$  and \*\*\* $P < 0.001$ . GPX7, glutathione peroxidase 7; oe, overexpression; NC, negative control.

Subsequently, the levels of ECM-related proteins were determined. GPX7 overexpression promoted the accumulation of the ECM components, aggrecan and collagen II, and reduced the levels of MMP13 and ADAMTS5, which are key enzymes involved in cartilage degradation (24). The experimental results indicated that GPX7 has the ability to regulate and inhibit the aforementioned pathogenic factors.

Increased chondrocyte apoptosis is a key manifestation of OA. In advanced-stage OA, chondrocytes become sparse and form cavities, and the ECM is also reduced due to chondrocyte apoptosis (25). It has been confirmed that in OA cartilage tissue, the apoptotic rate of chondrocytes is ~20% (26). Therefore, mechanisms through which to inhibit chondrocyte apoptosis has become a practical strategy in the treatment of OA. The present study demonstrated that the overexpression of GPX7 inhibited apoptosis, as shown using TUNEL staining and by the detection of apoptosis-related proteins. In addition, previous research has indicated that ferroptosis and apoptosis are closely linked, and ferroptosis promotes cell sensitivity to apoptosis (27). A previous study on stigmasterol demonstrated that inhibiting ferroptosis can alleviate IL-1 $\beta$ -induced chondrocyte damage and may have potential as a novel treatment for knee OA (28). Autophagic degradation of ferritin can cause chondrocyte ferroptosis and ECM degradation (29). High concentrations of iron can promote joint degeneration and promote the development of OA (30). Hence, the present study considered whether GPX7 can also affect ferroptosis. The detection of lipid peroxidation, ferrous ions and transporters revealed that GPX7 overexpression inhibited ferroptosis. An increasing number of studies have shown that ROS-induced lipid peroxidation is related to the pathogenesis of OA (31,32). Under pathological conditions, the intracellular cysteine metabolism pathway is blocked, indirectly inhibiting the activity of GPX4, thereby leading to the accumulation of lipid peroxides (33). The iron storage protein FTH1, which maintains iron homeostasis to prevent oxidative damage, decreases and transferrin receptors further enhance ferroptosis through additional uptake of iron-loaded Tf (34). In addition, inflammation, ECM degradation and apoptosis were promoted in the cells following treatment with the ferroptosis-inducing agent, erastin. This suggests that the regulatory role of GPX7 in these cell phenotypes may be partially mediated by a pathway involving ferroptosis. Erastin can also affect the biosynthesis of iron-sulfur clusters and thus mitochondrial function, interfering with cellular energy metabolism pathways and antioxidant systems (35). These combined mechanisms lead to changes in the response to erastin treatment and ultimately affect cell survival. Future detailed studies of these mechanisms will help to understand the role of GPX7 and erastin in ferroptosis and other cellular processes. In short, GPX4 has been widely recognized to be responsible for clearing peroxidized lipids, reducing cell damage, and delaying or inhibiting the occurrence of ferroptosis (36). Based on the results of the present study, GPX7 appears to be involved in inhibiting ferroptosis as well. However, the mechanisms through which GPX7 regulates ferroptosis specifically remain unclear. Additionally, the chondrocyte phenotypes cannot adequately represent the pathological environment of OA. Further research is required in the future to shed further light on this matter.

In conclusion, the present study reveals that GPX7 reduces IL-1 $\beta$ -induced chondrocyte inflammation, apoptosis and ECM degradation partially through a pathway involving ferroptosis. Exploring the association between OA and cell death may provide a theoretical basis and may enable the development of translational strategies for the treatment of OA. Future medicine development can target GPX7 (or the GPX family) and design compounds or biological agents to enhance or inhibit its activity. Screening and optimization of their modulators could lead to the development of medicine for modulating ferroptosis.

### Acknowledgements

Not applicable.

### Funding

The present study was supported by the Research Program of Teacher Education Curriculum Reform in Henan (grant no. 2024-JSJYYB-094), the Philosophy and Social Science Planning Program in Henan (grant no. 2021BTY006), and the Students' Innovation and Entrepreneurship Training Program in Henan University of Science and Technology (grant no. 2023461).

### Availability of data and materials

The data generated in the present study may be requested from the corresponding author.

### Authors' contributions

BC and WF designed and performed the experiments. CJ, GZ, ZL, YL and SZ participated in experiments and analyzed the data. BC wrote the manuscript. All authors read and approved the final manuscript. BC and WF confirm the authenticity of all the raw data.

### Ethics approval and consent to participate

Not applicable.

### Patient consent for publication

Not applicable.

### Competing interests

The authors declare that they have no competing interests.

### References

1. Yunus MHM, Nordin A and Kamal H: Pathophysiological perspective of osteoarthritis. *Medicina (Kaunas)* 56: 614, 2020.
2. Yao Q, Wu X, Tao C, Gong W, Chen M, Qu M, Zhong Y, He T, Chen S and Xiao G: Osteoarthritis: Pathogenic signaling pathways and therapeutic targets. *Signal Transduct Target Ther* 8: 56, 2023.
3. Hawker GA and King LK: The burden of osteoarthritis in older adults. *Clin Geriatr Med* 38: 181-192, 2022.
4. Katz JN, Arant KR and Loeser RF: Diagnosis and treatment of hip and knee osteoarthritis: A review. *JAMA* 325: 568-578, 2021.

5. Krause M, Freudenthaler F, Frosch KH, Achtnich A, Petersen W and Akoto R: Operative versus conservative treatment of anterior cruciate ligament rupture. *Dtsch Arztebl Int* 115: 855-862, 2018.
6. Molnar V, Matišić V, Kodvanj I, Bjelica R, Jeleč Ž, Hudetz D, Rod E, Čukelj F, Vrdoljak T, Vidović D, *et al.*: Cytokines and chemokines involved in osteoarthritis pathogenesis. *Int J Mol Sci* 22: 9208, 2021.
7. Xie Y, Kang R, Klionsky DJ and Tang D: GPX4 in cell death, autophagy, and disease. *Autophagy* 19: 2621-2638, 2023.
8. Kanemura S, Sofia EF, Hirai N, Okumura M, Kadokura H and Inaba K: Characterization of the endoplasmic reticulum-resident peroxidases GPx7 and GPx8 shows the higher oxidative activity of GPx7 and its linkage to oxidative protein folding. *J Biol Chem* 295: 12772-12785, 2020.
9. Wei PC, Hsieh YH, Su MI, Jiang X, Hsu PH, Lo WT, Weng JY, Jeng YM, Wang JM, Chen PL, *et al.*: Loss of the oxidative stress sensor NPGPx compromises GRP78 chaperone activity and induces systemic disease. *Mol Cell* 48: 747-759, 2012.
10. Hu X, Li B, Wu F, Liu X, Liu M, Wang C, Shi Y and Ye L: GPX7 Facilitates BMSCs Osteoblastogenesis via ER Stress and mTOR Pathway. *J Cell Mol Med* 25: 10454-10465, 2021.
11. Kim HJ, Lee Y, Fang S, Kim W, Kim HJ and Kim JW: GPx7 ameliorates non-alcoholic steatohepatitis by regulating oxidative stress. *BMB Rep* 53: 317-322, 2020.
12. Hwang HS and Shim JH: Brazilian and Caesalpinia sappan L. extract protect epidermal keratinocytes from oxidative stress by inducing the expression of GPX7. *Chin J Nat Med* 16: 203-209, 2018.
13. Zhou X, Zheng Y, Sun W, Zhang Z, Liu J, Yang W, Yuan W, Yi Y, Wang J and Liu J: D-mannose alleviates osteoarthritis progression by inhibiting chondrocyte ferroptosis in a HIF-2 $\alpha$ -dependent manner. *Cell Prolif* 54: e13134, 2021.
14. Zhou Y, Wu H, Wang F, Xu L, Yan Y, Tong X and Yan H: GPX7 Is Targeted by miR-29b and GPX7 knockdown enhances ferroptosis induced by erastin in glioma. *Front Oncol* 11: 802124, 2022.
15. Wang BW, Jiang Y, Yao ZL, Chen PS, Yu B and Wang SN: Aucubin protects chondrocytes against IL-1 $\beta$ -Induced apoptosis in vitro and inhibits osteoarthritis in mice model. *Drug Des Devel Ther* 13: 3529-3538, 2019.
16. Dixon SJ, Lemberg KM, Lamprecht MR, Skouta R, Zaitsev EM, Gleason CE, Patel DN, Bauer AJ, Cantley AM, Yang WS, *et al.*: Ferroptosis: An iron-dependent form of nonapoptotic cell death. *Cell* 149: 1060-1072, 2012.
17. Livak KJ and Schmittgen TD: Analysis of relative gene expression data using real-time quantitative PCR and the 2(-Delta Delta C(T)) Method. *Methods* 25: 402-408, 2001.
18. Guilak F, Nims RJ, Dicks A, Wu CL and Meulenbelt I: Osteoarthritis as a disease of the cartilage pericellular matrix. *Matrix Biol* 71-72: 40-50, 2018.
19. Wilkinson JM and Zeggini E: The genetic epidemiology of joint shape and the development of osteoarthritis. *Calcif Tissue Int* 109: 257-276, 2021.
20. Cui N, Hu M and Khalil RA: Biochemical and biological attributes of matrix metalloproteinases. *Prog Mol Biol Transl Sci* 147: 1-73, 2017.
21. Huang J, Zhao L and Chen D: Growth factor signalling in osteoarthritis. *Growth Factors* 36: 187-195, 2018.
22. Wang T and He C: Pro-inflammatory cytokines: The link between obesity and osteoarthritis. *Cytokine Growth Factor Rev* 44: 38-50, 2018.
23. Wang J, Chen J, Zhang B and Jia X: IL-6 regulates the bone metabolism and inflammatory microenvironment in aging mice by inhibiting Setd7. *Acta Histochem* 123: 151718, 2021.
24. Ashruf OS and Ansari MY: Natural compounds: Potential therapeutics for the inhibition of cartilage matrix degradation in osteoarthritis. *Life (Basel)* 13: 102, 2022.
25. Zhu R, Wang Y, Ouyang Z, Hao W, Zhou F, Lin Y, Cheng Y, Zhou R and Hu W: Targeting regulated chondrocyte death in osteoarthritis therapy. *Biochem Pharmacol* 215: 115707, 2023.
26. Zhang T and Li J: Experimental study on the ratios of chondrocytes apoptosis in OA. *Chin Modern Doctor* 46: 35-36, 2008 (In Chinese).
27. Mou Y, Wang J, Wu J, He D, Zhang C, Duan C and Li B: Ferroptosis, a new form of cell death: Opportunities and challenges in cancer. *J Hematol Oncol* 12: 34, 2019.
28. Mo Z, Xu P and Li H: Stigmasterol alleviates interleukin-1beta-induced chondrocyte injury by down-regulating sterol regulatory element binding transcription factor 2 to regulate ferroptosis. *Bioengineered* 12: 9332-9340, 2021.
29. Sun K, Hou L, Guo Z, Wang G, Guo J, Xu J, Zhang X and Guo F: JNK-JUN-NCOA4 axis contributes to chondrocyte ferroptosis and aggravates osteoarthritis via ferritinophagy. *Free Radic Biol Med* 200: 87-101, 2023.
30. Yang J, Hu S, Bian Y, Yao J, Wang D, Liu X, Guo Z, Zhang S and Peng L: Targeting cell death: Pyroptosis, ferroptosis, apoptosis and necroptosis in osteoarthritis. *Front Cell Dev Biol* 9: 789948, 2022.
31. Zhang X, Hou L, Guo Z, Wang G, Xu J, Zheng Z, Sun K and Guo F: Lipid peroxidation in osteoarthritis: Focusing on 4-hydroxynonenal, malondialdehyde, and ferroptosis. *Cell Death Discov* 9: 320, 2023.
32. An F, Zhang J, Gao P, Xiao Z, Chang W, Song J, Wang Y, Ma H, Zhang R, Chen Z and Yan C: New insight of the pathogenesis in osteoarthritis: The intricate interplay of ferroptosis and autophagy mediated by mitophagy/chaperone-mediated autophagy. *Front Cell Dev Biol* 11: 1297024, 2023.
33. Rochette L, Dogon G, Rigal E, Zeller M, Cottin Y and Vergely C: Lipid peroxidation and iron metabolism: Two corner stones in the homeostasis control of ferroptosis. *Int J Mol Sci* 24: 449, 2022.
34. Hou Y, Wang S, Jiang L, Sun X, Li J, Wang N, Liu X, Yao X, Zhang C, Deng H and Yang G: Patulin induces acute kidney injury in mice through autophagy-ferroptosis pathway. *J Agric Food Chem* 70: 6213-6223, 2022.
35. Cotticelli MG, Xia S, Lin D, Lee T, Terrab L, Wipf P, Huryn DM and Wilson RB: Ferroptosis as a novel therapeutic target for friedreich's Ataxia. *J Pharmacol Exp Ther* 369: 47-54, 2019.
36. Weaver K and Skouta R: The selenoprotein glutathione peroxidase 4: From molecular mechanisms to novel therapeutic opportunities. *Biomedicines* 10: 891, 2022.



Copyright © 2024 Chen et al. This work is licensed under a Creative Commons Attribution-NonCommercial-NoDerivatives 4.0 International (CC BY-NC-ND 4.0) License.